Magnetically recyclable $Fe^{3+}/TiO_2@Fe_3O_4$ nanocomposites towards degradation of direct blue 71 under visible-light irradiation

Abdollah Fallah Shojaei[1], *Ali Shams-Nateri*[2], *Maryam Ghomashpasand*[1] ✉

[1]*Department of Chemistry, Faculty of Science, University of Guilan, Rasht, P.O. Box 1914, Iran*
[2]*Textile Engineering Department, University of Guilan, P.O. Box: 41635-3756, Rasht, Iran*
✉ *E-mail: 2016maryamm@gmail.com*

Published in Micro & Nano Letters; Received on 7th October 2016; Revised on 2nd November 2016; Accepted on 14th November 2016

$Fe^{3+}/TiO_2@Fe_3O_4$ magnetic nanocompsites with 0.1–1 at% of Fe^{3+} content were synthesised by sol–gel method. The surface morphology, structure and crystalline phase of the nanocomposite were characterised by using XRD, SEM, HRTEM, EDX, BET, Diffuse reflectance spectroscopy (DRS) and VSM techniques. Photocatalytic activity experiments confirmed that as-prepared nanocomposite had good photodegradating behaviour to Direct Blue 71 under visible-light irradiation. 99.6% decomposition of dye was achieved within 50 min in the presence of the prepared photocatalyst. The nanocomposite could be easily recovered from the reaction solution by using a permanent magnetic bar and its photocatalytic activity remained 90% after five cycles of repetitious reusing. Then 0.5% $Fe^{3+}/TiO_2@Fe_3O_4$ nanocomposite can be used as highly efficient reusable catalysts.

1. Introduction: Organic dyes are widely used in various fields and severely induce water contamination. Most of the industrial dyes such as azo dyes are toxic and carcinogenic. The conventional techniques used for dyes removal are expensive, have average efficiency and secondary pollution [1]. Photodegradation is an useful method for environmental organic pollutants. Among several semiconductor photocatalysts, TiO_2 has been proved to be the most appropriate candidate for extensive environmental applications due to its biological and chemical inertness, high photocatalytic activity, inexpensiveness, non-toxicity, wide range of application, strong oxidising power and good physicochemical stability [2–4]. Even so, the practical application of TiO_2 slurry reactor is still limited mainly due to the trouble in separating TiO_2 nanoparticles from treated water. One solution of this problem is using of magnetically separable photocatalysts for the recovery and reuse of TiO_2 nanoparticles. Iron oxides have long been of interest for use in composites because of their combination of flexible surface functionalization, non-toxic nature and a sensitive magnetic response [5–8]. Unfavourable recombination rate of e^-/h^+ and low efficiency under irradiation in the visible region are the two other main disadvantages associated with the use of TiO_2 for environmental applications. Photocatalytic degradation of dyes with TiO_2 is performed under UV light irradiation, due to the wide band gap of the anatase form of TiO_2 (3.2 eV) [9]. Hence, extensive efforts have been made to modify TiO_2 with higher photocatalytic activity. Doping with metals or non-metal ions is a very effective effectiveness method to improve the charge separation and the visible photoactivity. Transition metal ions are used widely to trap charge carriers because they can effectively decrease the recombination rate of e^-/h^+ and reduction of band gap energy. A wide range of transition metal ions, such as Fe, Cu, La, Zr, W and Cr, have been used as dopants for TiO_2 [10–12]. Fe^{3+} ion is an interesting dopant to extend the absorption threshold towards visible range and has been most widely examined among these elements [13]. It is also believed that Fe^{3+} cations act as shallow traps in the titania lattices leading to their role in augmenting e^-/h^+ recombinations that expands the range of useful excitation light to the visible spectra. Taking into account therefore mentioned factors, the photodegradation mechanism can be affected when Fe^{3+} is incorporated into the catalyst [14, 15]. In the present investigation, a new magnetically separable $Fe^{3+}/TiO_2@Fe_3O_4$ core-shell nanocomposites were synthesised by sol–gel process to combine both advantages of Fe^{3+} and Fe_3O_4 and the photocatalytic activity was analysed by observing the mineralisation of Direct Blue 71 under visible-light illumination. The optimal Fe^{3+} dopant content, initial dye concentrations and catalyst dosage for effective photocatalytic reactivity has been studied.

2. Experimental

2.1. Synthesis of Fe_3O_4 nanoparticles: To synthesise of Fe_3O_4 magnetic nanoparticles, the mixture of $FeCl_2{\cdot}4H_2O$ (1.0 g) and $FeCl_3{\cdot}6H_2O$ (2.6 g) in a molar ratio of 1:2 were prepared by dissolving iron salts in 2.5 mL of HCl (2 M) solution. Then, 50 mL of ammonia aqueous solution (25%, v/v) was added into the solution with intensive stirring at room temperature under nitrogen gas protection. The Fe_3O_4 precipitate was produced immediately by adding ammonia aqueous. Finally, the particles washed three times with de-ionised water and dried at 60°C in an oven.

2.2. Synthesis of $Fe^{3+}/TiO_2@Fe_3O_4$ nanocomposites: The typical coating procedure was as follows: 1.44 g of Fe_3O_4 was dispersed in a mixed solution of 15.5 mL of glacial acetic acid and 8 mL of titanium tetreaisopropoxide (TTIP) and the mixture was stirred intensively for 30 min at room temperature. After that Fe $(NO_3)_3{\cdot}9H_2O$ (0.1, 0.3, 0.5, 0.8 and 1 at% with respect to TTIP) was dissolved in 170 mL of deionised water and this solution was added drop wise into the above sol with stirring. The mixture was stirred for 100 min at room temperature. The sol converted to gel by heating under oil-bath condition at 100°C for 1 h. The resulted gel was filtered, washed with deionized water and dried in an oven for several hours.

3. Results and discussion

3.1. Phase structures and morphology: The XRD patterns of prepared photocatalysts are shown in Fig. 1. As can be seen in Fig. 1*a*, all the diffraction peaks at 2θ: 25.2°, 37.8°, 47.9°, 54° and 62.6° of TiO_2 can be indexed to the TiO_2 anatase phase (JCPDS Card No. 21-1272). It can be seen in Fig. 1*b* that the relative intensity of (1 0 1) peaks decreased with the increase of Fe content significantly, indicating that the doped Fe could hinder obviously the increase of the TiO_2 crystallite size. Since the radius of Fe^{3+} is a little smaller than that of Ti^{4+}, the widening of (101) plane spacing indicates that some Fe^{3+} ions maybe enter to interstitial voids of TiO_2 lattice [16]. The diffraction peaks at

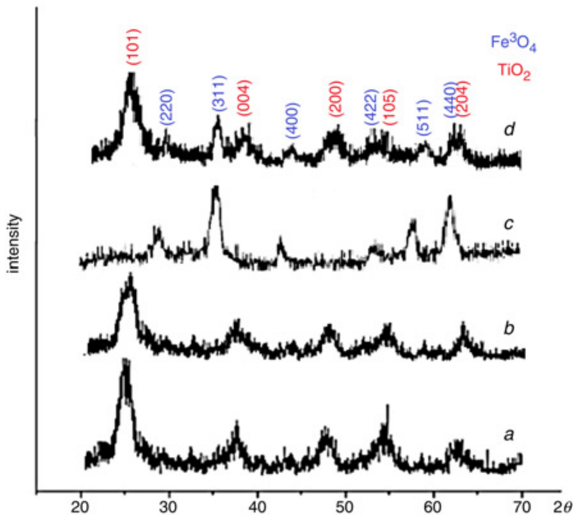

Fig. 1 *XRD patterns of samples*
a TiO_2
b 0.5% Fe^{3+}/TiO_2
c Fe_3O_4
d 0.5% $Fe^{3+}/TiO_2@Fe_3O_4$

around 30.1°, 35.4°, 43.0°, 53.4°, 56.9° and 62.0° were observed in Fig. 1*c* and could be assigned to diffraction of the face-centred cubic (fcc) lattice of Fe_3O_4 (JCPDS Card No. 79-0418). In Fig. 1*d*, the peaks related to the TiO_2 and Fe_3O_4 are still observed, which indicate the formation of 0.5% $Fe^{3+}/TiO_2@Fe_3O_4$ hybrid particles. The average dimensions of the 0.5% Fe^{3+}/TiO_2 and Fe_3O_4 nanoparticles are estimated about 8 and 20 nm, respectively, as calculated by using Scherrer's formula.

Fig. 2 gives the SEM and EDX photographs of 0.5% $Fe^{3+}/TiO_2@Fe_3O_4$ nanocomposite. The core–shell magnetic nanoparticles present nearly spherical shape with some degree of agglomeration and the average particle size is in the 30–50 nm range (Fig. 2*a*). The EDX spectrum (Fig. 2*b*) indicates the clear presence of Fe, O and Ti components. The strong Ti and O signals in the EDX spectrum show that TiO_2 surrounding the outer layer of the Fe_3O_4 core.

Fig. 3*a* shows the TEM image of the $TiO_2@Fe_3O_4$ nanocomposite particles. As shown in the micrograph, the core of the nanoparticle appears darker than the shell, which is identified to be Fe_3O_4 with average diameter about 20 nm. The average thickness of the shell layer (TiO_2) is measured to be about 5–8 nm. To obtain the detailed crystalline structure of the 0.5% $Fe^{3+}/TiO_2@Fe_3O_4$ magnetic nanocomposite, characterisation of HRTEM was carried out. In Fig. 3*b*, the lattice spacings of Fe_3O_4 is 0.29 nm, which corresponding to while that of TiO_2 is 0.35 nm. The core-shell structure can be clearly distinguished by the colour contrast between the cores and the shells. These observations indicate that the prepared hybrid particles possess distinct core-shell structure. After doping

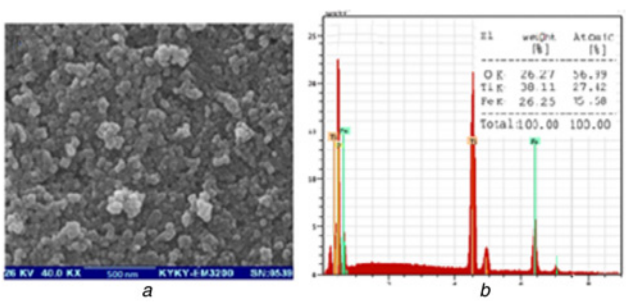

Fig. 2 *photographs of 0.5% $Fe^{3+}/TiO_2@Fe_3O_4$ a) SEM and b) EDX*

Fe, the 0.5% Fe^{3+}/TiO_2 shell decrease in thickness (about 2–5 nm). This signifies that doping of Fe might have decreased the *d*-spacing of TiO_2 and the length.

DRS can be presented some perception into the interactions of the photocatalyst with photon energies. The reflectance spectra of pure TiO_2, 0.5% Fe^{3+}/TiO_2 and 0.5% $Fe^{3+}/TiO_2@Fe_3O_4$ samples are illustrated in Fig. 4. Pure TiO_2 only absorbed ultraviolet radiation of <400 nm. The UV–visible spectra of the Fe-doped TiO_2 powders were obtained to determine the relationship between the solar energy conversion efficiency and the spectroscopic property (Fig. 4).

In the spectra of 0.5% Fe/TiO_2, the absorption bands was somewhat shifted to a longer wavelength compared with pure TiO_2, and the broadened tail may indicate a Fe component. The band gap obtained by extrapolation in pure TiO_2 and 0.5% Fe^{3+}/TiO_2 was about 3.2 and 2.7 eV (Table 1), respectively.

The band gap in a semiconductor is closely related to the wavelength range absorbed, where the band gap decreases with increasing absorption wavelength. The 0.5% $Fe^{3+}/TiO_2@Fe_3O_4$ nanocomposite exhibited in the visible-light region of 400–700 nm. This led to the reduction of the band gap. The band gaps for 0.5% $Fe^{3+}/TiO_2@Fe_3O_4$ nanocomposite are 2.6 eV.

3.2. Photocatalytic activity: To evaluate the photoactivity of the $Fe^{3+}/TiO_2@Fe_3O_4$ nanocomposites for degradation of Direct Blue 71 and determine the optimum amount of Fe doping, experiments carried out by different Fe amounts of doped samples ranging from 0.1 to 1 at% for 50 min, and the results are given in Fig. 5. It demonstrates that the photocatalytic activities increase with the increasing of Fe concentration and the order was as follows: 0.5 at%> 0.3 at% > 0.8 at% > 1 at% > 0.1 at%. Then, the 0.5% $Fe^{3+}/TiO_2@Fe_3O_4$ has the highest efficiency. The Fe dopants can serve as a charge traps retarding the e^-/h^+ recombination rate and enhancing the interfacial charge transfer to degrade the dye within the suitable concentration range of dopant (0.5 at%). When the dopant concentration is too high, the recombination rate will increase leading to the obvious decrease in the removal capacity.

Fig. 6 compares the photocatalytic activities of pure TiO_2, 0.5% Fe^{3+}/TiO_2, $TiO_2@Fe_3O_4$ and 0.5% $Fe^{3+}/TiO_2@Fe_3O_4$

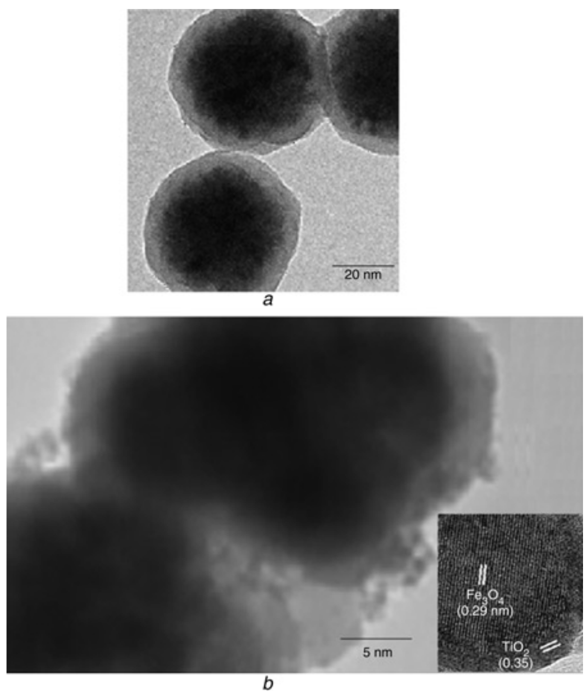

Fig. 3 *TEM image of*
a TiO_2/Fe_3O_4 and HRTEM of
b 0.5% $Fe^{3+}/TiO_2@Fe_3O_4$

Micro & Nano Letters, 2017, Vol. 12, Iss. 3, pp. 161–165
doi: 10.1049/mnl.2016.0620

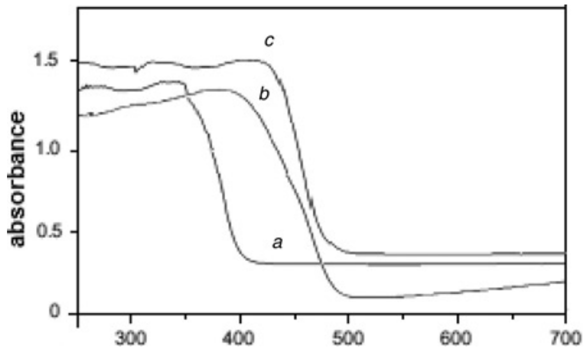

Fig. 4 *UV–vis diffuse reflectance spectra of*
a TiO_2
b 0.5% Fe^{3+}/TiO_2
c 0.5% $Fe^{3+}/TiO_2@Fe_3O_4$

Table 1 Summary of physical properties of prepared nanoparticles

Sample	Band gap wavelength, nm	Band gap energy, eV	Specific surface area, m^2g^{-1}	Pore volume, cm^3g^{-1}
TiO_2	384	3.2	62	0.19
0.5% Fe/TiO_2	462	2.7	89	0.31
0.5% $Fe^{3+}/TiO_2@Fe_3O_4$	474	2.6	137	0.52

nanoparticles. The dye solutions were kept in the dark for 30 min by stirring to reach the adsorption equilibrium. The results indicate that there is no significant dye decomposition without light irradiation. The saturated adsorption rate is in good agreement with the BET surface areas of the synthesised nanocomposites without irradiation (Table 1). The photodegradation efficiency of prepared samples increased in the order: 0.5% $Fe^{3+}/TiO_2@Fe_3O_4$ > 0.5% Fe^{3+}/TiO_2 > $TiO_2@Fe_3O_4$ > pure TiO_2. This higher efficiency of the doped catalysts is attributed to the intense absorption in the visible-light region and Fe^{3+} can act as both hole and electron traps to enhance lifetimes of electrons and holes. The photo-generated charge carriers can be transferred into different surface sites where they will react with adsorbed dye and enhance photo-catalytic activity. Another reason is the small size of the anatase nanocrystals of the shell by Fe^{3+} doping, that making the 0.5% $Fe^{3+}/TiO_2@Fe_3O_4$ microspheres possess high-specific surface, thus they can effectively adsorb more molecules and also offer more reaction sites. In addition, Fe_3O_4 nanoparticles can also affect the photocatalytic activity of the synthesised material.

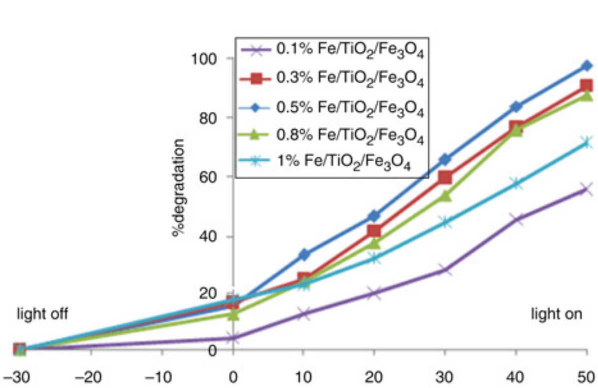

Fig. 5 *Photodegradation of Direct Blue 71 by $Fe^{3+}/TiO_2@Fe_3O_4$ nanocomposites with different Fe^{3+} contents in dark and under visible-light (pH = 7, catalyst = 30 mg L^{-1}, dye = 50 mg L^{-1} and T = 25°C)*

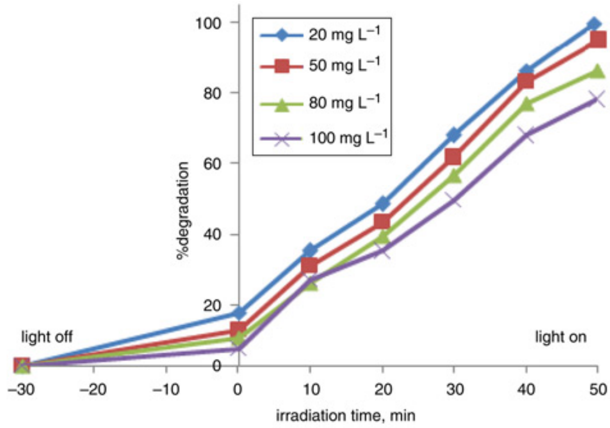

Fig. 6 *The effect of initial dye concentration on the photodegradation of Direct Blue 71 in presence of 0.5% $Fe^{3+}/TiO_2@Fe_3O_4$ in dark and under visible-light (pH = 7, catalyst = 30 mg L^{-1} and T = 25°C)*

Therefore, the doped catalysts could absorb visible-light and to be activated to generate electron–hole pairs which would participate directly in the photocatalytic reactions.

3.3. Effect of catalyst loading: To investigate the effect of 0.5% $Fe^{3+}/TiO_2@Fe_3O_4$ catalyst loading on the degradation rate of Direct Blue 71, experiments were conducted for four different catalyst loadings as 10, 20, 30 and 40 mg L^{-1}, at initial dye concentration of 50 mg L^{-1} for 50 min irradiation time. The obtained results have been shown in Fig. 7. It can be seen that the extent of degradation of dye increased significantly by increase the catalyst dosage up to a concentration of 30 mg L^{-1} (99.6%) and then begins to decrease gradually. It can be pointed out that, the photodecomposition rates of pollutants are influenced by the active sites and the photoabsorption of the catalyst used in the study. At higher loadings, the catalysts may block the light irradiation, and restrain the effective usage of light for photo excitation.

3.4. Effect of initial dye concentration: The photocatalytic degradation of Direct Blue 71 was carried out at various initial concentrations of 20, 50, 80 and 100 mg L^{-1} (Fig. 8). The experiments have been conducted by 30 mg L^{-1} catalyst loading for 50 min visible-light irradiation time.

When the initial dye concentration was increased from 20 to 100 mg L^{-1}, the dye removal efficiency was decreased from 99.9% to 80%.

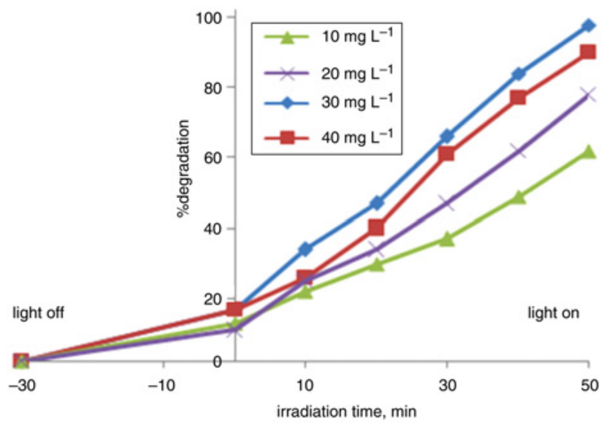

Fig. 7 *Photodegradation of Direct Blue 71 in presence of different amount of 0.5% $Fe^{3+}/TiO_2@Fe_3O_4$ in dark and under visible-light (pH = 7, dye = 50 mg L^{-1} and T = 25°C)*

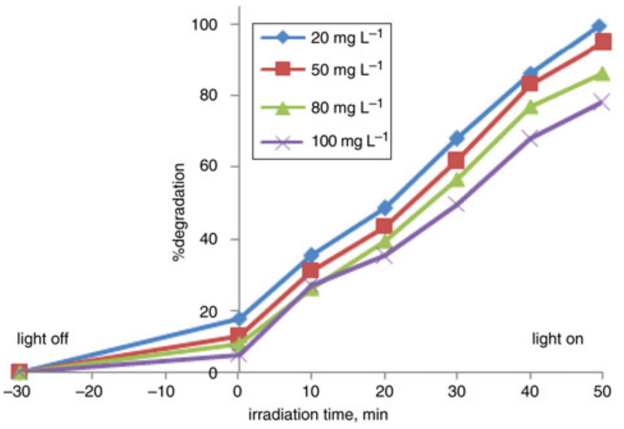

Fig. 8 *The effect of initial dye concentration on the photodegradation of Direct Blue 71 in presence of 0.5% $Fe^{3+}/TiO_2@Fe_3O_4$ in dark and under visible-light (pH = 7, catalyst = 30 mg L^{-1} and T = 25°C)*

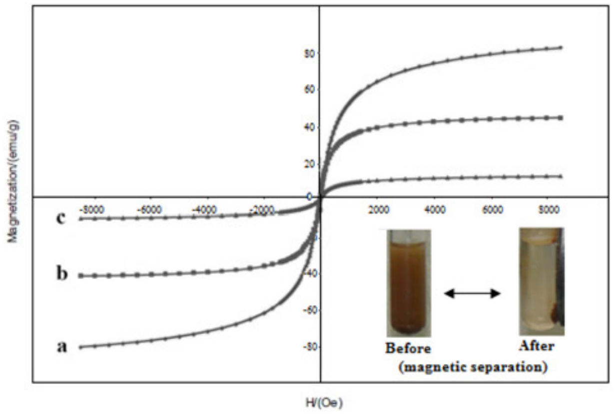

Fig. 9 *The magnetic properties of nanoparticles*
a Fe_3O_4
b TiO_2/Fe_3O_4
c 0.5% $Fe^{3+}/TiO_2@Fe_3O_4$

An explanation to this behaviour is that as the initial concentration of dye increases, more organic substances adsorbed on the catalytic surface. Therefore, generation of $OH^{\bullet}$ will be reduced, since there are only a fewer active sites for the adsorption of hydroxyl ions and the generation of hydroxyl radicals. At high dye concentrations, the active sites are covered by dye ions. Therefore, the absorption of photons and consequently the photocatalytic efficiency is reduced.

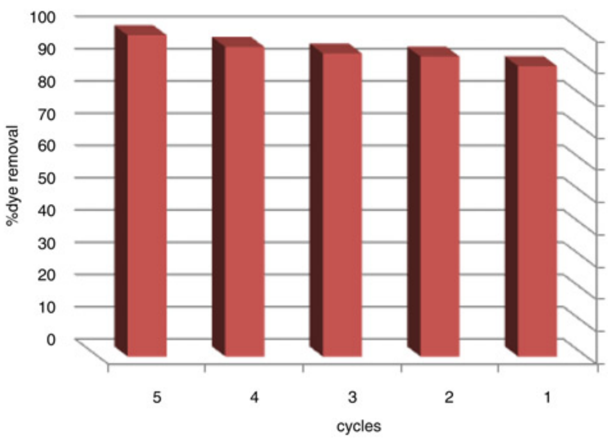

Fig. 10 *Photodegradation of Direct Blue 71 in presence of 0.5% $Fe^{3+}/TiO_2@Fe_3O_4$ under visible-light after five repetitive use (pH = 7, catalyst = 30 mg L^{-1}, T = 25°C and t = 50 min for each cycle)*

3.5. Magnetic and recovery properties: For recovery and reuse of nanocatalysts, magnetic nanocomposite that possesses super paramagnetic behaviour at room temperature is preferred. To evaluate the magnetic response of the nanocomposites to an external field, the saturation magnetisation (M_s) was measured. The maximum saturation magnetisations of Fe_3O_4, $TiO_2@Fe_3O_4$ and 0.5% $Fe^{3+}/TiO_2@Fe_3O_4$ were 81.8, 12.9 and 41.6 emu g^{-1}, respectively, as shown in Figs. 9a–c. The data indicate that all samples are superparamagnetic. The reduced magnetisation is still sufficiently strong to ensure good performance during magnetic recovery.

Fig. 10 shows the efficiency photocatalytic degradation of the 0.5% $Fe^{3+}/TiO_2@Fe_3O_4$ nanocomposite after being used for five times. It can be observed that the photocatalytic activity of Direct Blue 71 has no noticeable decrease and the efficiency of catalyst is remained about 90%.

4. Conclusion: In summary, $Fe^{3+}/TiO_2@Fe_3O_4$ magnetic nanocomposites as the novel catalyst with 0.1–1 at% of Fe^{3+} content were successfully prepared by sol–gel method. The nanoparticles were characterised using XRD, SEM, EDX, HRTEM, BET, DRS and VSM techniques. The iron doping caused the new absorption band to appear in the visible region and affected on the photocatalysis activity. The photocatalytic activity of $Fe^{3+}/TiO_2@Fe_3O_4$ nanocomposite was compared with pure TiO_2, Fe^{3+}/TiO_2 and $TiO_2@Fe_3O_4$ nanoparticles towards the degradation of Direct Blue 71 under visible-light irradiation. The results showed that >99% decomposition of dye was achieved within 50 min in optimum condition. The recycling photocatalytic experiment showed that the separated magnetic nanoparticles have a good photocatalytic activity after five cycles of repetitive use.

5. Acknowledgment: The authors are grateful to University of Guilan for financial assistance.

6 References

[1] Chung Y.C., Chen C.Y.: 'Degradation of azo dye reactive violet 5 by TiO_2 photocatalysis', *Environ. Chem. Lett.*, 2009, **7**, pp. 347–352

[2] Zou J., Gao J., Xie F.: 'An amorphous TiO_2 sol sensitized with H_2O_2 with the enhancement of photocatalytic activity', *J. Alloys Compd.*, 2010, **497**, pp. 420–427

[3] Tseng Y.H., Liu S., Kuo C.S., *ET AL.*: 'Preparation of nano-sized TiO_2 sol and its visible-light-responsive photocatalysis in aquatic state', *Micro Nano Lett.*, 2006, **1**, pp. 116–119

[4] Fallah Moafi H., Fallah Shojaie A., Zanjanchi M.A.: 'The comparison of photocatalytic activity of synthesized TiO_2 and ZrO_2 nanosize onto wool fibers', *Appl. Surf. Sci.*, 2010, **256**, pp. 4310–4316

[5] Yao K.F., Peng Z., Liao Z.H., *ET AL.*: 'Preparation and photocatalytic property of TiO_2-Fe_3O_4 core-shell nanoparticles', *J. Nanosci. Nanotechnol.*, 2009, **9**, pp. 1458–1461

[6] Xu S., Shangguan W., Yuan J., *ET AL.*: 'Preparations and photocatalytic properties of magnetically separable nitrogen-doped TiO_2 supported on nickel ferrite', *Appl. Catal. B Environ.*, 2007, **71**, pp. 177–184

[7] Fallah-Shojaei A., Tabatabaeian K., Shirini F., *ET AL.*: 'Multi-walled carbon nanotube supported Fe_3O_4 NPs: an efficient and reusable catalyst for the one-pot synthesis of 4H-pyran derivatives', *R. Soc. Chem. Adv.*, 2014, **4**, (4), pp. 9509–9516

[8] Hu X., Yang J., Zhang J.: 'Magnetic loading of $TiO_2/SiO_2/Fe_3O_4$ nanoparticles on electrode surface for photoelectrocatalytic degradation of diclofenac', *J. Hazard. Mater.*, 2011, **196**, pp. 220–227

[9] Alvarez P.M., Jaramillo J., Lopez-Pioero F., *ET AL.*: 'Preparation and characterization of magnetic TiO_2 nanoparticles and their utilization for the degradation of emerging pollutants in water', *Appl. Catal. B Environ.*, 2010, **100**, pp. 338–345

[10] Yadav H.M., Otari S.V., Koli V.B., *ET AL.*: 'Preparation and characterization of copper-doped anatase TiO_2 nanoparticles with visible light

doi: 10.1049/mnl.2016.0620

photocatalytic antibacterial activity', *J. Photochem. Photobiol. A Chem.*, 2014, **280**, pp. 32–38

[11] Li X., Chen Z., Shi Y., ET AL.: 'Preparation of N, Fe co-doped TiO_2 with visible light response', *Powder Technol.*, 2011, **207**, pp. 165–169.

[12] Pozan Soylu G.S., Isleyen M., Gokcen S.: 'Transition metal coated TiO_2 nanoparticles: synthesis, characterization and their photocatalytic activity', *Appl. Catal. B Environ.*, 2013, **140–141**, pp. 537–545

[13] Zhu J., Chen F., Zhang J., ET AL.: 'Fe3+-TiO2 photocatalysts prepared by combining sol–gel method with hydrothermal treatment and their characterization', *J. Photochem. Photobiol. A Chem.*, 2006, **180**, pp. 196–204

[14] Tang W., Chen X., Xia J., ET AL.: 'Preparation of an Fe-doped visible-light-response TiO_2 film electrode and its photoelectrocatalytic activity', *Mater. Sci. Eng. B*, 2014, **187**, pp. 39–45

[15] Song X., Yang F., Fang Q., ET AL.: 'Capsule-like CdS-modified TiO_2 nanocomposites with enhanced photodegradation under visible light irradiation', *Micro Nano Lett.*, 2015, **10**, pp. 157–160

[16] Wen L., Liu B., Zhao X., ET AL.: 'Synthesis, characterization, and photocatalysis of Fe-doped TiO_2: A combined experimental and theoretical study', *Int. J. Photoenergy*, 2012, **2012**, pp. 368750–368760

[17] Habibi M.H., Tangestaninejad S., Fallah-Shojaie A.: 'Photolytic recovery of inorganic mercury compounds as mercury poisoning or environmental pollutants by complexation with N-(2-methyl-phenyl) 4-nitro-thiobenzamide ligand', *Fresenius Environ. Bull.*, 2005, **14**, pp. 2–9.